Supporting Information

Ce ions and polyaniline co-intercalation into MOF-derived porous V_2O_5 nanosheets with synergistic energy storage mechanism for high-capacity and super-stable aqueous zinc-ion batteries

Yibo Zhang[a,b], Zhihua Li[a,b,*], Bo Zhao[a,b], Ziyi Wang[a,b] amd Jun Liu[a]

[a] School of Materials Science and Engineering, Central South University, Changsha, 410083, P.R. China.

[b] Key Laboratory of Nonferrous Metal Materials Science and Engineering of Ministry of Education, Central South University, Changsha 410083, P.R. China.

* **Corresponding author.**

E-mail address: ligfz@csu.edu.cn (Z. Li).

Experimental section

Materials

Vanadium(III) chloride (VCl_3, 97%), terephthalic acid (H_2BDC, 99%), cerium(III) nitrate hexahydrate ($Ce(NO_3)_3·6H_2O$, 99.5%), aniline (99.5%), hydrogen peroxide (H_2O_2, 30%), *N*-methyl-2-pyrrolidone (NMP, 99.5%), poly(vinylidene fluoride) (PVDF) and zinc trifluoromethanesulfonate ($Zn(CF_3SO_3)_2$, 98%) were purchased from Aladdin Chemicals (Shanghai, China). *N,N*-dimethylformamide (DMF, 99.5%), hydrochloric acid (HCl, 48%), methanol (99.5%) and absolute ethanol (99.5%) were supplied from Adamas-beta (Shanghai, China).

Materials preparation

Synthesis of V-MOF and porous V_2O_5: In the V-MOF synthesis procedure,[28] a mixture of VCl_3 (473 mg, 3 mmol), H_2BDC (498 mg, 3 mmol), DMF (50 mL) were stirred vigorously for 30 min. Afterwards, the resulting mixture was heated in a 100 mL Teflon-lined stainless steel autoclave at 180 °C for 12 h. The dark green product (V-MOF) was centrifuged and washed several times with methanol solution, followed by drying in a vacuum oven for 12 h at 60 °C. Finally, the porous V_2O_5 was obtained by annealing V-MOF at 350 °C for 2 h with a ramping rate of 2 °C min^{-1} under air atmosphere.

Synthesis of Ce/PANI/V_2O_5 nanocomposites: The Ce ions and PANI co-intercalated V_2O_5 was synthesized by a facile hydrothermal method.[26] Typically, the newly synthesized porous V_2O_5 (182 mg, 1 mmol) and H_2O_2 (1 mL) were dispersed in 30 mL deionized water. After stirring at 30 °C for 30 min, $Ce(NO_3)_3·6H_2O$ (87 mg, 0.2 mmol) and aniline (90 μL) were simultaneously added into the above mixture and magnetically stirred for another 60 min. Subsequently, the mixture was transferred into an autoclave and heated at 120 °C for 24 h. The final products (Ce/PANI/V_2O_5 nanocomposites) were collected by centrifugation and then washed several times with deionized water, and the obtained sample was named as CPVO. For comparison, the Ce/V_2O_5 composite was prepared by the same method without the addition of aniline, and denoted as CVO.

Materials characterization

The phase composition and crystal structure of the as-prepared samples were analyzed by X-ray powder diffraction (XRD, Bruker D8 Advance, Germany). The microstructure of the samples was investigated by scanning electron microscopy (SEM, ZEISS Sigma 300, Germany) and transmission electron microscopy (TEM, FEI Titan G2 60-300, USA). The chemical composition and valence state of the products were characterized by X-ray photoelectron spectroscopy (XPS, Thermo Scientific K-Alpha, USA). The functional groups of the as-synthesized samples were further characterized by Fourier transform infrared spectroscopy (FT-IR, Nicolet 6700, USA). The specific surface area and pore distribution of the samples were measured on a surface area porosity analyzer (ASAP 2020, Micromeritics, USA).

Electrochemical Analysis

The as-synthesized active materials, acetylene black and PVDF were weighed at a mass ratio of 7:2:1, and uniformly ground in NMP to obtain a mixed slurry. Subsequently, the obtained slurry was evenly coated on the stainless steel mesh and dried at 60 °C overnight in a vacuum oven to form the working electrode. The mass loading of the active material on the current collector was around 2.0 mg cm^{-2}. The CR2032 coin cell was assembled by using the above working electrode as the cathode, high-purity zinc foil (12 mm diameter) as the anode, glass fiber membrane (Whatman, GF/D) as the separator and 3 M $Zn(CF_3SO_3)_2$ as the aqueous electrolyte, respectively. The galvanostatic charge-discharge (GCD) and galvanostatic intermittent titration technique (GITT) tests were measured on a battery testing system (Neware, CT-4008). The cyclic voltammetry (CV) and electrochemical impedance spectroscopy (EIS) measurements were conducted on an electrochemical workstation (CHI 760E).

Computational methods

All the theoretical calculations were investigated by using the Vienna ab initio simulation package (VASP).[19] The electron-ion interactions were analyzed by the projected augmented wave (PAW) method, and the electron exchange and correlation interactions were determined by the Perdew-Burke-Ernzerhof (PBE) functional. For all the calculated results, the energy cut-off for the plane-wave basis set was 500 eV. All structures were optimized according to the convergence criteria of energy and force of

10^{-5} e V and 0.02 eV/Å, respectively. A vacuum thickness of 15 Å was used to prevent the nonphysical interactions between periodic images, while the van der Waals interactions were corrected employing the Grimme (D3).[27] For the Brillouin zone sampling, a 2 × 2 × 3 and 2 × 2 × 1 Monkhorst-Pack mesh grid was utilized for CVO and CPVO composites. The electronic properties of CVO system were reasonably described by an on-site Coulomb interaction with the effective parameter U – J = 4.0 eV (for V ions) or 5.0 eV (for Ce ions), respectively.

References

19 Y. Zhang, Z. Li, L. Gong, X. Wang, P. Hu and J. Liu, *J. Energy Chem.*, 2023, **77**, 561–571.

26 W. He, Z. Fan, Z. Huang, X. Liu, J. Qian, M. Ni, P. Zhang, L. Hu and Z. Sun, *J. Mater. Chem. A*, 2022, **10**, 18962–18971.

27 S. Liu, H. Zhu, B. Zhang, G. Li, H. Zhu, Y. Ren, H. Geng, Y. Yang, Q. Liu and C.C. Li, *Adv. Mater.*, 2020, **32**, 2001113.

28 Y. Zhang, Z. Li, M. Liu and J. Liu, *Chem. Eng. J.*, 2023, **463**, 142425.

Figures and Tables:

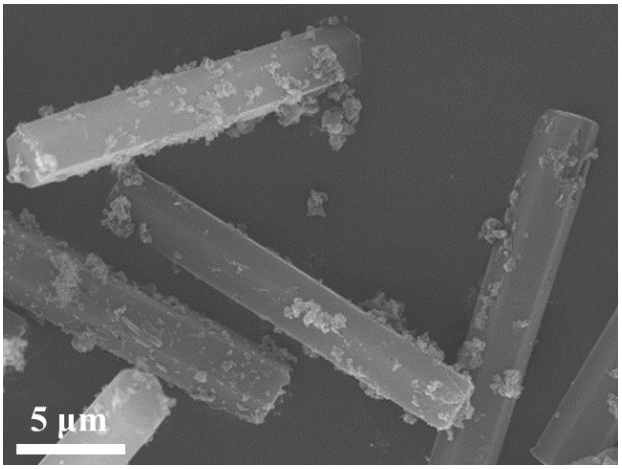

Fig. S1. SEM image of V-MOF.

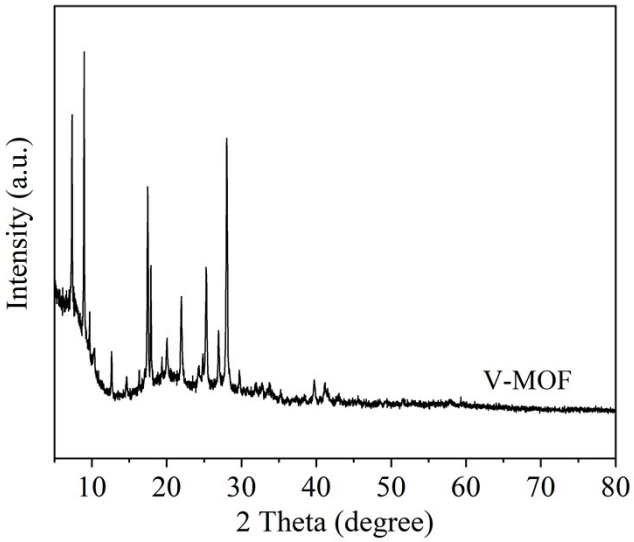

Fig. S2. XRD pattern of V-MOF.

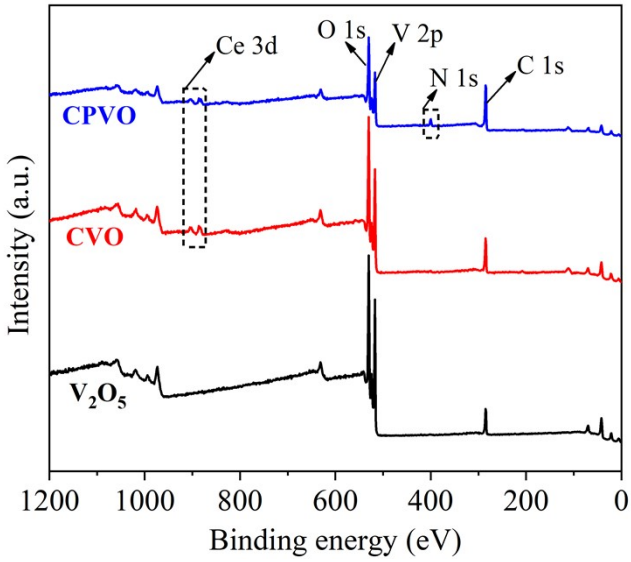

Fig. S3. The survey XPS spectrum of the as-derived V_2O_5, CVO and CPVO.

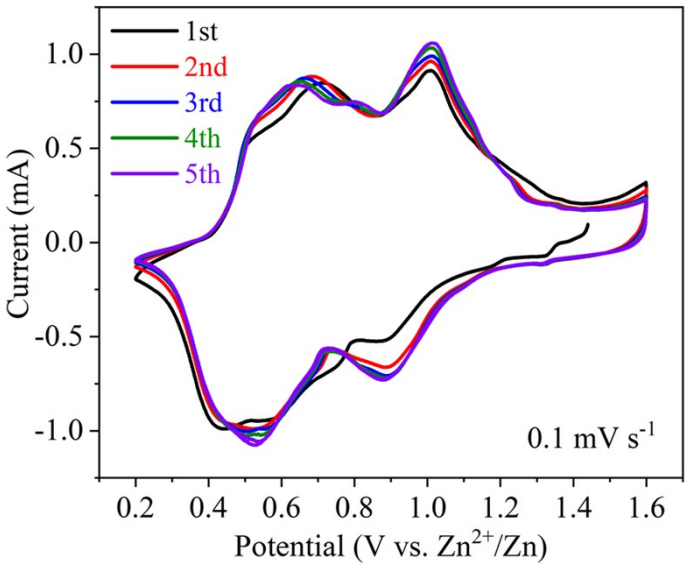

Fig. S4. Initial five CV curves of the CPVO electrode at a scanning rate of 0.1 mV s^{-1}.

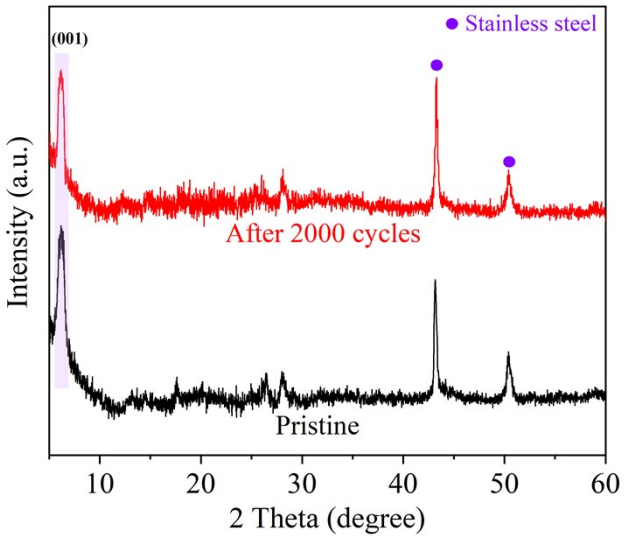

Fig. S5. The XRD patterns of CPVO before and after the cycles.

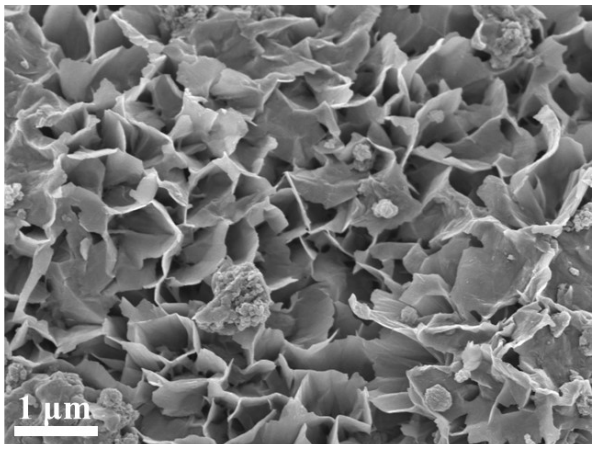

Fig. S6. SEM images of CPVO after 2000 cycles at 10.0 A g^{-1}.

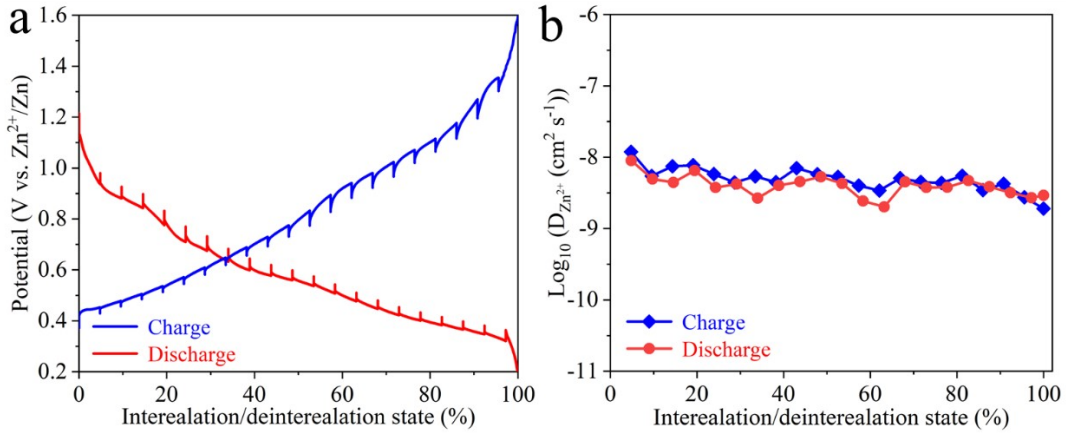

Fig. S7. (a) The charge-discharge GITT profiles of the CVO electrode at 0.1 A g^{-1}. (b) The calculated Zn^{2+} diffusion coefficients (D_{Zn}^{2+}) of CVO electrode in the charge-discharge process.

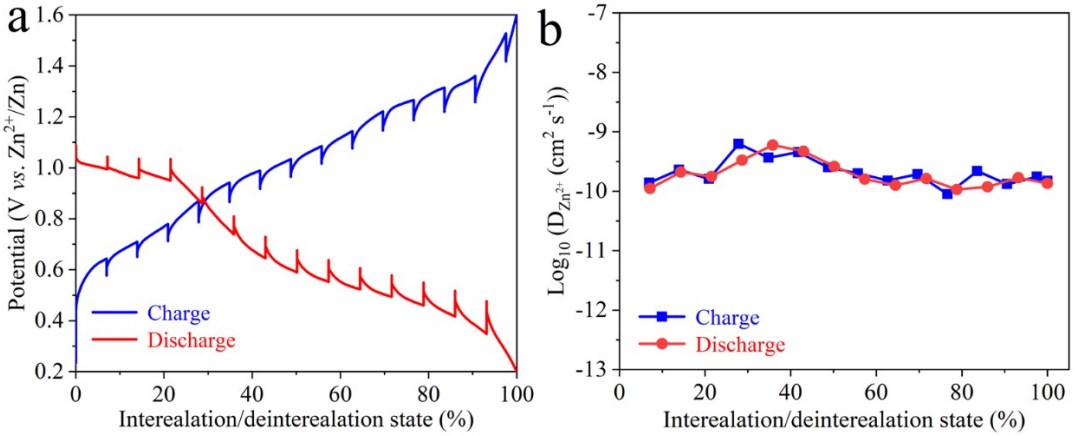

Fig. S8. (a) The charge-discharge GITT profiles of the V_2O_5 electrode at 0.1 A g^{-1}. (b) The calculated Zn^{2+} diffusion coefficients (D_{Zn}^{2+}) of V_2O_5 electrode in the charge-discharge process.

Table S1. Inductively coupled plasma optical emission spectrometer (ICP-OES) result of CPVO.

Sample	Ce (mg/g)	V (mg/g)	Ce (wt.%)	V (wt.%)	Ce/V (wt.%)
CPVO	52.43	387.62	5.24	38.76	13.52

Table S2. The comparison of electrochemical performance of various vanadium-based electrodes.

Cathode material	Capacity	Current density	Cycling stability	Capacity retention
O_d-Ce@V_2O_5 [24]	~285 mAh g^{-1}	5.0 A g^{-1}	900 cycles	~44.6%
PANI-V_2O_5 [27]	264.6 mAh g^{-1}	10.0 A g^{-1}	1000 cycles	95.3%
(1Zn, 1Ch)-VOH [43]	263 mAh g^{-1}	4.0 A g^{-1}	2000 cycles	91%
$KMgV_2O_5 \cdot nH_2O$ [44]	318 mAh g^{-1}	4.0 A g^{-1}	2000 cycles	72%
$Cs_{0.24}V_2O_5 \cdot 0.19H_2O$ [45]	269.7 mAh g^{-1}	10.0 A g^{-1}	5000 cycles	99.5%
NaNVO-PANI [46]	267 mAh g^{-1}	5.0 A g^{-1}	5000 cycles	92%
$NH_4V_3O_8 \cdot 0.5H_2O$ [47]	276.1 mAh g^{-1}	10.0 A g^{-1}	1000 cycles	95%
MnVOH@PEDOT [48]	334.3 mAh g^{-1}	5.0 A g^{-1}	2000 cycles	84.8%
CPVO nanosheets (this work)	**316.8 mAh g^{-1}**	**10.0 A g^{-1}**	**2000 cycles**	**93.8%**

References

24 M. Bao, Z. Zhang, X. An, J. Liu, J. Feng, B. Xi and S. Xiong, *Nano Res.*, 2023, **16**, 2445–2453.

27 S. Liu, H. Zhu, B. Zhang, G. Li, H. Zhu, Y. Ren, H. Geng, Y. Yang, Q. Liu and C.C. Li, *Adv. Mater.*, 2020, **32**, 2001113.

43 Q. Zong, Y. Zhuang, C. Liu, Q. Kang, Y. Wu, J. Zhang, J. Wang, D. Tao, Q. Zhang and G. Cao, *Adv. Energy Mater.*, 2023, **13**, 2301480.

44 Z. Feng, Y. Zhang, J. Sun, Y. Liu, H. Jiang, M. Cui, T. Hu and C. Meng, *Chem. Eng. J.*, 2022, **433**, 133795.

45 H. Liu, X. Hou, T. Fang, Q. Zhang, N. Gong, W. Peng, Y. Li, F. Zhang and X. Fan, *Energy Storage Mater.*, 2023, **55**, 279–288.

46 S. Zhao, S. Wang, J. Guo, L. Li, C. Li, Y. Sun, P. Xue, D. Wu, L. Wei, Y. Wang and Q. Zhang, *Adv. Funct. Mater.*, 2023, **33**, 2305700.

47 Y. Li, Y. Liu, J. Chen, Q. Zheng, Y. Huo, F. Xie and D. Lin, *Chem. Eng. J.*, 2022, **448**, 137681.

48 S. Tan, Z. Sang, Z. Yi, J. Guo, X. Zhang, P. Li, W. Si, J. Liang and F. Hou, *EcoMat.*, 2023, **5**, e12326.